IOPscience iopscience.iop.org

Home Search Collections Journals About Contact us My IOPscience

Structure and thermal stability of δ-Bi_2O_3 thin films deposited by reactive sputtering

This article has been downloaded from IOPscience. Please scroll down to see the full text article.

2006 J. Phys. D: Appl. Phys. 39 1939

(http://iopscience.iop.org/0022-3727/39/9/032)

View the table of contents for this issue, or go to the journal homepage for more

Download details:
IP Address: 202.127.206.107
The article was downloaded on 30/06/2010 at 03:07

Please note that terms and conditions apply.

Institute of Physics Publishing | Journal of Physics D: Applied Physics
J. Phys. D: Appl. Phys. **39** (2006) 1939–1943 doi:10.1088/0022-3727/39/9/032

Structure and thermal stability of δ-Bi_2O_3 thin films deposited by reactive sputtering

H T Fan, S S Pan, X M Teng, C Ye and G H Li[1]

Key Laboratory of Materials Physics, Anhui Key Laboratory of Nanomaterials and Nanotechnology, Institute of Solid State Physics, Chinese Academy of Sciences, Hefei 230031, People's Republic of China

E-mail: ghli@issp.ac.cn

Received 20 January 2006
Published 20 April 2006
Online at stacks.iop.org/JPhysD/39/1939

Abstract
Nanocrystalline δ-Bi_2O_3 thin films have been deposited onto Si (100) and quartz substrates by reactive sputtering. The structural characteristics and thermal stability of the thin films have been investigated by x-ray diffraction and Raman spectra. It was found that the δ-Bi_2O_3 thin films could exist stably below 200 °C and undergo a phase transition sequence $\delta \to \beta \to \alpha$ with increasing annealing temperature beyond 200 °C. These phase transitions were further confirmed by optical constant and optical band gap studies.

(Some figures in this article are in colour only in the electronic version)

1. Introduction

Bismuth oxide has attracted great attention in recent years because of its unique optical and electrical properties, which make Bi_2O_3 films well suited to applications in various domains such as optoelectronics, sensor technology, optical coatings, solid oxide fuel cell and ceramic glass manufacturing [1–10].

Bismuth oxide has five main polymorphic forms that are labelled as α-, β-, γ-, δ- [11] and ω-Bi_2O_3 phase [12]. Each polymorph possesses different crystalline structures and various electrical, optical and mechanical properties. The face-centred cubic δ-Bi_2O_3 is stable over a narrow range 729–825 °C. The cooling down of the high temperature δ-Bi_2O_3 phase leads to the formation of intermediate metastable phases such as tetragonal β-Bi_2O_3 and/or body-centred cubic γ-Bi_2O_3 before transforming into stable monoclinic α-Bi_2O_3 at room temperature (RT) [13, 14]. δ-Bi_2O_3 could be stabilized at low temperature by doping with different transition metal oxides or rare earth [15], but pure δ-Bi_2O_3 thin films have not been obtained at RT for a long time. Recently, δ-Bi_2O_3 thin films have been synthesized by electrodeposition [16] and chemical vapour deposition (CVD) [17]. Compared with electrodeposition and CVD methods, magnetron sputtering is often employed to fabricate various thin films due to a greater variety of substrates, environmentally friendly starting materials and relatively high film quality.

In general, the operation temperature at which many electric or optical devices made of δ-Bi_2O_3 thin film, such as solid oxide fuel cell work is above RT. Also a fluctuation in the working temperature of the practical devices is inevitable, so the thermal behaviours of the films have to be fully evaluated before their applications in many potential fields. In our previous study [18], the fabrication details and optical properties of as-grown thin films have been reported. In this paper, we present the structural characterization and thermal stability of as-grown δ-Bi_2O_3 thin films by heat-treating at different temperatures.

2. Experiment

The as-grown δ-Bi_2O_3 thin films were deposited by radio frequency (RF) reactive sputtering onto Si (100) and quartz at 200 °C, with O_2 flow ratio [O_2/(O_2+Ar)] at about 5%. The fabrication details can be found in our previous report [18]. δ-Bi_2O_3 thin films were annealed at temperatures ranging from 200 to 500 °C for 1 h in a tube furnace in air with a heating rate of about 6 °C min^{-1} and then naturally cooled down to RT in furnace.

The crystalline structure was analysed by grazing angle x-ray diffraction (XRD) measurements achieved with a Philips X'Pert Pro MPD diffractometer, using Cu-Kα radiation. A confocal laser micro-Raman spectrometer (LABRM-HR) was used to obtain Raman spectra in the reflection mode using an Ar^+ laser with a 514.5 nm radiation at RT. The

[1] Author to whom any correspondence should be addressed.

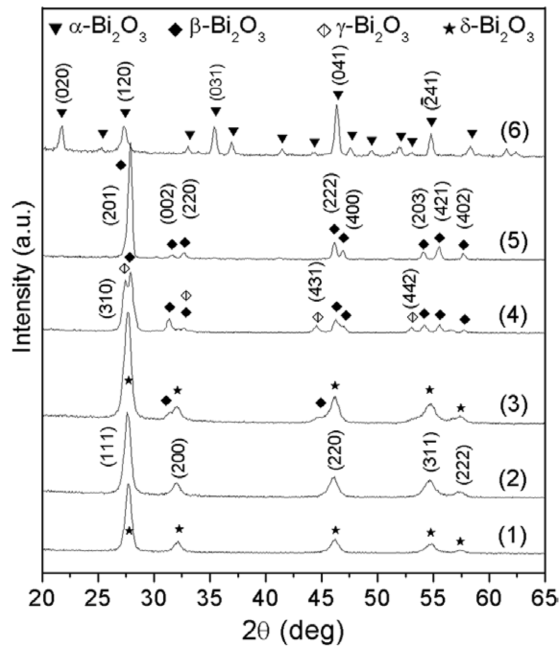

Figure 1. XRD patterns of as-grown and annealed δ-Bi_2O_3 thin films at different temperatures: (1) as-grown, (2) 200 °C, (3) 250 °C, (4) 300 °C, (5) 400 °C and (6) 500 °C.

Surface morphologies were observed using a Sirion 200 field emission scan electron microscope (FE-SEM) operating with an accelerating voltage of 5 kV. The optical constants were analysed using a spectroscopic ellipsometer (UVISEL JOBIN-YVON). A Varian spectrophotometer (CARY-5E) was used to record the absorption spectra.

3. Results and discussions

Figure 1 shows the XRD patterns of the as-grown and annealed δ-Bi_2O_3 thin films deposited onto Si (100) substrates at different temperatures. The XRD profiles of the samples deposited onto quartz (not presented here) are similar to those deposited onto Si substrates. All the XRD patterns reported here have been analysed by appealing to the International Centre for Diffraction Data (ICCD) database for the Bi_2O_3 phase (41-1449, 78-1793, 45-1344 and 52-1007 for α, β, γ and δ phase, respectively). From curve (1) in figure 1, one can see that all the diffraction peaks of the as-grown thin film can be indexed as δ-Bi_2O_3. The diffraction peaks of the sample annealed at 200 °C are the same as the as-grown one, and no peak shift or other diffraction peaks are observed, as shown in curve (2) in figure 1. In fact, even after annealing at 200 °C for over 4 h, the FCC structure still remains, indicating a very high thermal stability of the δ-Bi_2O_3 thin film. Some shoulders on the diffraction peaks of the δ-Bi_2O_3 phase could be observed when annealed at 250 °C, as shown in curve (3) in figure 1. According to the standard ICCD patterns for Bi_2O_3, the shoulders can be identified as β-Bi_2O_3, indicating the partial decomposition of δ-Bi_2O_3 into β-Bi_2O_3 took place at 250 °C, which was caused by thermodynamic metastability of the δ-Bi_2O_3 phase at low temperature [19]. Generally, as a nonequilibrium phase at low temperature the δ-Bi_2O_3 phase tends to transform into a more stable phase upon annealing treatment. For example, a transition from $Bi_2O_{2.33}$ to Bi_2O_3 after annealing has been reported for chemically deposited bismuth oxide thin films by Gujar *et al* [20]. By increasing annealing temperature to 300 °C, the phase transition from δ to β proceeded and a new phase transition from δ to γ was triggered simultaneously. The coexistence of the diffraction peaks ascribed to the β and γ phases confirms the formation of a phase mixture of β-Bi_2O_3 and γ-Bi_2O_3, see curve (4) in figure 1. It has been reported that the intermediate metastable β-Bi_2O_3 phase exists stably in a wide temperature range 330–650 °C in the phase transition sequence from δ-Bi_2O_3 to α-Bi_2O_3 [13]. When annealed at 400 °C, a pure β-Bi_2O_3 phase was formed; see curve (5) in figure 1. In our experiments, the stable existence of the β-Bi_2O_3 phase is considered to be due to the nanocrystalline nature of the thin film [16, 21]. By further increasing annealing temperature to 500 °C, recrystallization of the δ-Bi_2O_3 nanocrystallite occurs, and the nanocrystalline characteristic, which stabilizes the metastable phase in thin films, could not work any more. It is believed that the recrystallization gives rise to the phase transition ($\delta \rightarrow \beta \rightarrow \alpha$ or $\beta \rightarrow \alpha$) of the Bi_2O_3 thin films during annealing and/or cooling down to RT.

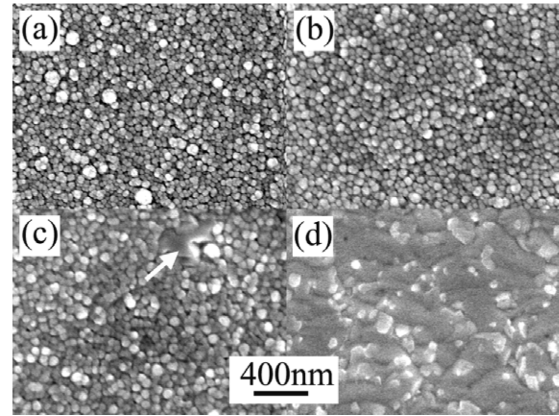

Figure 2. SEM images of as-grown and annealed Bi_2O_3 thin films at different temperatures: (*a*) as-grown, (*b*) 300 °C, (*c*) 400 °C and (*d*) 500 °C.

SEM observations were carried out to investigate the surface morphology evolution of Bi_2O_3 thin films upon annealing treatment. No obvious morphology change was observed for the δ-Bi_2O_3 thin films when annealed at temperature below 300 °C as compared with the as-grown one, as shown in figures 2(*a*) and (*b*). These two films have a uniform structure and fine crystallites, and the average grain size of as-grown film is approximately 20 nm and increases slightly upon annealing at 300 °C. When annealed at 400 °C, instead of regular and uniform crystallites, some irregular and abnormal grown crystallites (marked by arrow) are found, (see figure 2(*c*)). In spite of visible differences in the grain shape as compared with the as-grown thin films, the average grain size of the film annealed at 400 °C is still in nanometre scale, about 50 nm, and this nanocrystalline nature is considered still the main reason for the presence of metastable β-Bi_2O_3 at RT. The nanocrystalline feature of the films annealed at 500 °C almost disappears, as shown in figure 2(*d*). The dissolution of grain boundary indicated the occurrence of recrystallization of the δ-Bi_2O_3 phase. Due to relatively high atom mobility at

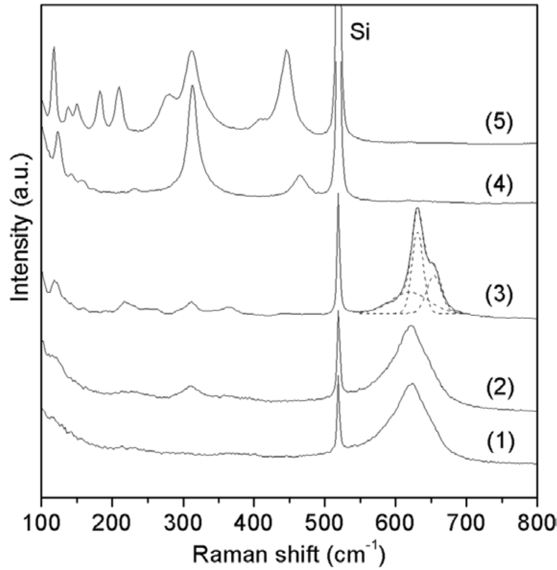

Figure 3. Raman spectra of annealed Bi_2O_3 thin films at different temperatures: (1) 200 °C, (2) 250 °C, (3) 300 °C, (4) 400 °C and (5) 500 °C.

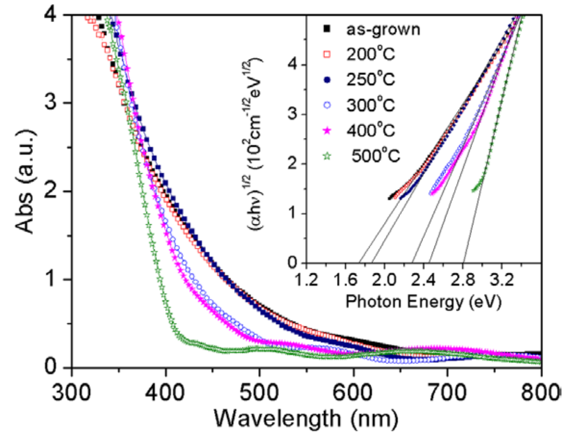

Figure 4. Absorption spectra of as-grown and annealed Bi_2O_3 thin films at different temperatures. The inset is a plot of $(\alpha h\nu)^{1/2}$ versus $h\nu$.

high temperature, the most stable phase, α-Bi_2O_3, would be obtained inevitably after cooling down to RT.

Figure 3 shows the Raman spectra of Bi_2O_3 thin films annealed at different temperatures. The peak located at 519.2 cm^{-1} corresponds to the first-order optical phonon mode of c-Si substrate [22]. δ-Bi_2O_3 has a defective-fluorite structure with a very high level of deficiency in oxygen sublattice [23]. Crystals with fluorite structure of space group Fm3m (O_h^5) are characterized by a simple vibrational structure with only one Raman active phonon of T_{2g} symmetry at $k = 0$ [24]. Indeed, there is only one broadened peak at 618 cm^{-1} in the Raman spectrum for the film annealed at 200 °C, see curve (1) in figure 3, which is similar to that of the as-grown δ-Bi_2O_3 films [18] and close to the reported value [25]. This indicates that the annealed thin film has the same phase component with the as-grown one. The additional weak band at 312 cm^{-1}, which is present in the film annealed at 250 °C and higher, is consistent with the XRD result, indicating that a second phase appears. The Raman spectrum of the thin film annealed at 300 °C is very different from that of the as-grown one; see curve (3) in figure 3. Several weak peaks located at 121, 218, 312 and 365 cm^{-1} and a broadened band appear, and the broadened band can be deconvoluted with three frequencies, i.e. 618, 631 and 655 cm^{-1}. The Raman band occurring at 618 cm^{-1} belongs to the δ-Bi_2O_3 phase, indicating that decomposition of the δ-Bi_2O_3 phase at 300 °C is not completed. The Raman shifts at 121 and 312 cm^{-1} can be assigned to β-Bi_2O_3 due to the existence of β-Bi_2O_3 according to XRD result. The actual assignments of Raman peaks at 218, 365, 631 and 655 cm^{-1} remain uncertain and require further study, whereas a possible assignment for them is that they originate from γ-Bi_2O_3, identified by XRD analyses. When annealed at 400 °C, see curve (4) in figure 3, three strong Raman frequencies located at 121, 312, 465 cm^{-1} and two weak frequencies at 142 and 158 cm^{-1} can be seen and are consistent with the Raman spectrum of β-Bi_2O_3 reported in the literature [26]. A typical α-Bi_2O_3 Raman spectrum [4] is obtained for the film annealed at 500 °C, indicating that the δ-Bi_2O_3 has completely transformed into α-Bi_2O_3 during annealing. This result is in good agreement with XRD measurement.

Figure 4 shows the absorption spectra for the as-grown and annealed thin films. In the region of the fundamental absorption edge, the energy dependences of the absorption coefficient, α, are given by the following equation:

$$\alpha h\nu = A(h\nu - E_g)^n, \quad (1)$$

where $h\nu$ is the incident photon energy, A is a characteristic parameter independent of photon energy, E_g is optical band gap and n is an index that characterizes the optical absorption process and is theoretically equal to 1/2 and 2 for direct allowed and indirect allowed transitions, respectively. According to the above equation, in the vicinity of the fundamental absorption edge, $(\alpha h\nu)^2$ and $(\alpha h\nu)^{1/2}$ linearly depend upon the photon energy for direct and indirect allowed transitions, respectively. Therefore, by extrapolating the respective linear part to the zero value of the ordinate, one can obtain the value of E_g from the intercept of abscissa for direct and indirect transitions. From the analysis of experimental absorption curves, it was found that the indirect allowed transition is predominant in Bi_2O_3 thin films since the best plot which covers the widest range of data is obtained for the indirect allowed transition. To apply this relation for the samples under investigation, $(\alpha h\nu)^{1/2}$ as a function of $h\nu$ are plotted and illustrated in the inset of figure 4 for α larger than 10^4 cm^{-1}. For the indirect allowed transition, E_g is found to be about 1.73, 1.86, 2.26, 2.45 and 2.81 eV for the thin films annealed at 200 °C, 250 °C, 300 °C, 400 °C and 500 °C, respectively. The band gap of the thin film annealed at 200 °C is equal to that of the as-grown one, indicating that annealing at 200 °C has no notable effect on the optical band gap of the as-grown δ-Bi_2O_3 thin film. By increasing the annealing temperature, the E_g value of Bi_2O_3 thin films increases gradually. The change in band gaps of the annealed thin films originates from the existence of different phases in Bi_2O_3 films. It is worth noting that the band gaps of the films annealed at 400 and 500 °C, corresponding to pure β-Bi_2O_3 and α-Bi_2O_3, are 2.45 eV and 2.81 eV, respectively. The band gap for the α-Bi_2O_3 phase obtained here is larger than that obtained from α-Bi_2O_3 powders [10]. Based on the

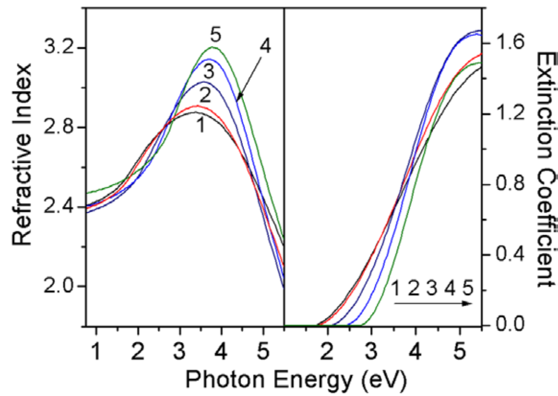

Figure 5. Refractive indices and extinction coefficients of as-grown and annealed Bi_2O_3 thin films at different temperatures: (1) as-grown, (2) 200 °C, (3) 300 °C, (4) 400 °C and (5) 500 °C.

XRD and Raman analyses, the thin films annealed at 250 °C and 300 °C are a mixture of two phases ($\delta+\beta$) and three phases ($\delta+\beta+\gamma$), respectively, and thus the optical band gap increases with the increase in annealing temperature.

The Tauc-Lorentz (TL) model [27, 28] was adopted to describe the dispersion of Bi_2O_3 thin films. A simple four layers stack structure, Si/SiO_2/Bi_2O_3/(Bi_2O_3+Void), was employed to extract the optical constants of thin films. The thicknesses of SiO_2, Bi_2O_3 and (Bi_2O_3+Void) layers for the as-grown film after fitting are 5.8 nm, 297.4 nm, and 18.7 nm respectively. One can see that the layers of SiO_2 and (Bi_2O_3+Void) are very thin as compared with Bi_2O_3 layer. By increasing annealing temperature the thickness of SiO_2 interfacial layer increases slightly due to the reaction between the Bi_2O_3 layer and the Si substrate during high temperature annealing. A similar observation has been reported for the Ta_2O_5/Si system by Ono *et al* [29]. The refractive indices and extinction coefficients of the as-grown and annealed thin films extracted from the best-fitted results are shown in figure 5. It is apparent that the extrema of the refractive index increase with increasing annealing temperature and move slightly towards high photon energy region. The refractive index and extinction coefficient are closely related to the density of materials [30], being higher at higher density. The gradual reduction of the void in the films with increasing annealing temperature, as shown in the FESEM images in figure 2, is evidence of the increased density of the annealed films. A slight increase in the refractive index and extinction coefficient for the thin film annealed at 200 °C is due to the increase in the stacking density upon annealing. An obvious variation of optical constants for the thin film annealed at 300 °C has been observed and is considered to be due to its phase mixture structure, and the increase in refractive index probably originates from the partial phase transition from δ-Bi_2O_3 to β-Bi_2O_3 due to the higher refractive index of the pure β-Bi_2O_3 phase than the δ-Bi_2O_3 phase, as can be seen from curve (4) in figure 5. The densification and scattering effects in nanocrystalline Bi_2O_3 thin films are also responsible for the increase of the extinction coefficient. For the thin film annealed at 500 °C with a pure α-Bi_2O_3, the refractive index has the maximum value over the whole photon energy range and the extinction coefficients are lower than all the other films in the low energy region. This is in agreement with the gradual change in the transparency of the films from the as-grown brownish translucence into yellowish transparency with increasing annealing temperature.

4. Conclusions

In summary, δ-Bi_2O_3 thin films have been deposited onto Si (100) and quartz substrates by reactive sputtering and annealed at temperatures ranging from 200 to 500 °C. The XRD analyses proved that δ-Bi_2O_3 phase could exist stably below 200 °C and transform completely to β-Bi_2O_3 and α-Bi_2O_3 after annealing at 400 °C and 500 °C, respectively. XRD and Raman results demonstrated that the δ-Bi_2O_3 thin films undergo a phase transformation sequence $\delta \rightarrow \beta \rightarrow \alpha$ with increasing annealing temperature. SEM observations revealed the nanocrystalline nature of δ-Bi_2O_3 and β-Bi_2O_3 thin films, which (is believed) accounts for the stability of non-equilibrium phases (δ and β) at RT. The indirect transition optical band gaps of Bi_2O_3 thin films increase with increasing annealing temperature following the hierarchy E_g, $\delta < \beta < \alpha$, for different phases. The extremum of the refractive index increases with increasing annealing temperature and moves slightly towards higher photon energy region. The phase transition and densification with increasing annealing temperature are responsible for the significant change in optical constants upon annealing treatment.

Acknowledgment

This work was supported by the National Key Project of Fundamental Research for Nanomaterials and Nanostructures (No 2005CB623603).

References

[1] Leontie L, Caraman M, Visinoiu A and Rusu G I 2005 *Thin Solid Films* **473** 230
[2] Leontie L, Caraman M, Alexe M and Harnagea C 2002 *Surf. Sci.* **507** 480
[3] Lei M, Li S T 1, Jiao X D, Li J Y and Alim M A 2004 *J. Phys. D: Appl. Phys.* **37** 804
[4] Devi G S, Manorama S V and Rao V J 1998 *J. Electrochem. Soc.* **145** 1039
[5] Gujar T P, Shinde V R, Lokhande C D, Mane R S and Han Sung-Hwan 2006 *Appl. Surf. Sci.* **252** 2747
[6] Chakravorty D and Mathews T 1989 *J. Phys. D: Appl. Phys.* **22** 149
[7] Fuentes O R, Aguilera E S, Velasquez C, Alvarado R O, Alonso J C and Ortiz A 2005 *Thin Solid Films* **478** 96
[8] Clapham P B 1967 *Brit. J. Appl. Phys.* **18** 363
[9] Holland L and Siddall G 1958 *Brit. J. Appl. Phys.* **9** 359
[10] Chakrabarti M, Dutta S, Chattapadhyay S, Sarkar A, Sanyal D and Chakrabarti A 2004 *Nanotechnology* **15** 1792
[11] Sammes N M, Tompsett G A, Näfe H and Aldinger F 1999 *J. Eur. Ceram. Soc.* **19** 1801
[12] Gualtieri A F, Immovilli S and Prudenziati M 1997 *Powder Diffract* **12** 90
[13] Shuk P, Wiemhöfer H -D, Guth U, Göpel W and Greenblatt M 1996 *Solid State Ion.* **89** 179
[14] Harwig H A 1977 *Thesis* State University Utrecht
[15] Kharton V V, Naumovich E N, Yaremchenko A A and Marques F M B 2001 *J. Solid State Electrochem.* **5** 160
[16] Switzer J A, Shumsky M G and Bohannan E W 1999 *Science* **284** 293
[17] Takeyama T, Takahashi N, Nakamura T and Itoh S 2005 *J. Cryst. Growth* **275** 460

[18] Fan H T, Teng X M, Pan S S, Ye C, Li G H and Zhang L D 2005 *Appl. Phys. Lett.* **87** 231916
[19] Yaremchenko A A, Kharton V V, Naumovich E N and Tonoyan A A 2000 *Mater. Res. Bull.* **35** 515
[20] Gujar T P, Shinde V R, Lokhande C D, Mane R S and Han Sung-Hwan 2005 *Appl. Surf. Sci.* **250** 161
[21] Helfen A, Merkourakis S, Wang G, Walls M G, Roy E, Yu-Zhang K and Wang Y L 2005 *Solid State Ion.* **176** 629
[22] Hart T R, Aggarwal R L and Lax B 1970 *Phys. Rev.* B **1** 638
[23] Yashima M and Ishimura D 2003 *Chem. Phys. Lett.* **378** 395
[24] Keramidas V G and White W B 1973 *J. Chem. Phys.* **59** 1561
[25] Skorodumova N V, Jonsson A K, Herranen M, Strømme M, Niklasson G A, Johansson B and Simak S I 2005 *Appl. Phys. Lett.* **86** 241910
[26] Hardcastle F D and Wachs I E 1992 *J. Solid State Chem.* **97** 319
[27] Jellison G E Jr and Modine F A 1996 *Appl. Phys. Lett.* **69** 371
[28] Jellison G E Jr and Modine F A 1996 *Appl. Phys. Lett.* **69** 2137
[29] Ono and Koyanagi K 1999 *Appl. Phys. Lett.* **75** 3521
[30] Sangwal K and Kucharczyk W 1987 *J. Phys. D: Appl. Phys.* **20** 522